JNS

LABORATORY INVESTIGATION

# Live-cell imaging to detect phosphatidylserine externalization in brain endothelial cells exposed to ionizing radiation: implications for the treatment of brain arteriovenous malformations

**Zhenjun Zhao, PhD,[1] Michael S. Johnson, PhD,[2] Biyi Chen,[1] Michael Grace, BMedPhys,[3] Jaysree Ukath, MSc,[3] Vivienne S. Lee, BLabMed,[1] Lucinda S. McRobb, PhD,[1] Lisa M. Sedger, PhD,[1] and Marcus A. Stoodley, PhD[1]**

[1]Department of Clinical Medicine, Faculty of Medicine and Health Sciences, Macquarie University; [2]Faculty of Science, University of Technology; and [3]Genesis Cancer Care, Macquarie University Hospital, Sydney, New South Wales, Australia

**OBJECT** Stereotactic radiosurgery (SRS) is an established intervention for brain arteriovenous malformations (AVMs). The processes of AVM vessel occlusion after SRS are poorly understood. To improve SRS efficacy, it is important to understand the cellular response of blood vessels to radiation. The molecular changes on the surface of AVM endothelial cells after irradiation may also be used for vascular targeting. This study investigates radiation-induced externalization of phosphatidylserine (PS) on endothelial cells using live-cell imaging.

**METHODS** An immortalized cell line generated from mouse brain endothelium, bEnd.3 cells, was cultured and irradiated at different radiation doses using a linear accelerator. PS externalization in the cells was subsequently visualized using polarity-sensitive indicator of viability and apoptosis (pSIVA)-IANBD, a polarity-sensitive probe. Live-cell imaging was used to monitor PS externalization in real time. The effects of radiation on the cell cycle of bEnd.3 cells were also examined by flow cytometry.

**RESULTS** Ionizing radiation effects are dose dependent. Reduction in the cell proliferation rate was observed after exposure to 5 Gy radiation, whereas higher radiation doses (15 Gy and 25 Gy) totally inhibited proliferation. In comparison with cells treated with sham radiation, the irradiated cells showed distinct pseudopodial elongation with little or no spreading of the cell body. The percentages of pSIVA-positive cells were significantly higher ($p = 0.04$) 24 hours after treatment in the cultures that received 25- and 15-Gy doses of radiation. This effect was sustained until the end of the experiment (3 days). Radiation at 5 Gy did not induce significant PS externalization compared with the sham-radiation controls at any time points ($p > 0.15$). Flow cytometric analysis data indicate that irradiation induced growth arrest of bEnd.3 cells, with cells accumulating in the G2 phase of the cell cycle.

**CONCLUSIONS** Ionizing radiation causes remarkable cellular changes in endothelial cells. Significant PS externalization is induced by radiation at doses of 15 Gy or higher, concomitant with a block in the cell cycle. Radiation-induced markers/targets may have high discriminating power to be harnessed in vascular targeting for AVM treatment.

http://thejns.org/doi/abs/10.3171/2015.4.JNS142129

**KEY WORDS** phosphatidylserine externalization; endothelial cells; ionizing radiation; brain arteriovenous malformations; live-cell imaging; cell cycle; stereotactic radiosurgery; vascular disorders

Brain arteriovenous malformations (AVMs) are congenital abnormalities that consist of direct connections between arteries and veins, allowing high-pressure arterial blood to flow into fragile cerebral veins, resulting in a high risk of hemorrhagic stroke.[16,37] The aim of AVM treatment is to prevent hemorrhage.[29] Treatment is effective only with complete AVM removal or obliteration.[14] Current treatments—namely surgery, endovascular occlusion, or stereotactic radiosurgery—are all associated with significant limitations.[1,42] The surgical risk is generally unacceptable for lesions that are large, located in critical brain structures, or involve deep perforating arter-

**ABBREVIATIONS** AVM = arteriovenous malformation; FWD = forward; PI = propidium iodide; PS = phosphatidylserine; pSIVA = polarity-sensitive indicator of viability and apoptosis; SRS = stereotactic radiosurgery.

**SUBMITTED** September 15, 2014. **ACCEPTED** April 7, 2015.
**INCLUDE WHEN CITING** Published online October 2, 2015; DOI: 10.3171/2015.4.JNS142129.

ies. Endovascular treatment is usually not able to achieve a complete obliteration and is used to facilitate surgery rather than attempt cure.[1]

Stereotactic radiosurgery (SRS), a technique to deliver focused ionizing radiation to the AVM tissues in the brain, has been widely used to treat these patients.[11,30] SRS can focus on the targeted nidus precisely, with only negligible amounts of radiation delivered to the surrounding brain tissue.[30] The margin dose of the radiation is typically 16–25 Gy, depending on the nidus size, location, shape, and proximity to critical structures.[10,44] Occlusion rates are generally greater than 70%.[44]

The purpose of SRS for AVMs is to occlude the blood vessels. The processes of AVM vessel occlusion after radiosurgery are poorly understood but are believed to involve a combination of cellular proliferation and intravascular thrombosis.[3,36] Unfortunately, there is a delay to occlusion of 2–3 years after treatment and the risk of hemorrhage is not reduced until complete obliteration occurs.[12,13] Another problem with SRS is that the radiation dose must be selected carefully so that it is not too high, which may cause radiation-induced injury to surrounding tissues, or too low, which may not be sufficient to cause obliteration of the vessels.[9] Although SRS scoring systems have been developed and validated in clinical practice,[31] understanding the biological response of endothelium to radiation may permit a more accurate prediction of SRS outcomes. Radiation-induced changes in some cells, such as cancer cells, have been investigated;[17,18,34] however, the relevant studies in brain endothelial cells are limited, especially at the molecular level.

The molecular changes on the surface of AVM endothelial cells after radiation treatment may also be used as targets for vascular targeting (i.e., delivering thrombotic agents selectively to AVM sites by targeting markers on these cells, with the goal of obliterating the AVM vessels rapidly by inducing thrombosis).[25,33,38] A highly discriminating target, which dominantly expresses on AVM endothelium, is required for the success of this technique. We have investigated the molecular characteristics of the endothelial surface of AVM vessels[20,39,40] and, although differences were found in comparison with normal blood vessels, no target with adequate discriminating power has been found to date. However, radiation-induced molecular changes on the endothelial surface may be a promising source of targets for vascular targeting.[4] Due to its ability to deliver precisely focused radiation beams, the SRS-induced molecular changes can be restricted within the AVMs.

It is well known that ionizing radiation can cause DNA damage and may lead to cell apoptosis.[35] Cell damage can induce phosphatidylserine (PS) externalization on the membrane.[7,26] Indeed, PS has been widely used as a marker of cell injury.[26] Results of our previous work indicated that PS was externalized selectively in the AVM nidus after radiosurgery in an AVM animal model and that PS is a potential molecular target for vascular targeting.[38] More comprehensive study of PS externalization after radiosurgery is required to reveal the molecular response of endothelial cells induced by radiation and its feasibility as a target for vascular targeting.

The conventional way to study PS externalization is to use fluorescently labeled annexin V, a protein that selectively binds to PS as a reporter molecule. Normally, cultured cells or tissue slides are stained with annexin conjugates and the cells analyzed by microscopy or flow cytometry.[26] However, because PS is a constructional lipid component of the cell membrane that is normally located on the inner surface of the membrane, many experimental treatments, such as harvest or fixation, can cause PS externalization.[43,45] Hence, the results may not be reliable. Advances in microscopy have led to the development of live-cell imaging in recent years,[32] and this represents an ideal method to observe PS externalization, because cell staining and monitoring are performed during culture. The technique allows for the visual detection of dynamic changes of PS externalization in real time after stimulation. Furthermore, it is a simple technique in which cells do not require any treatment except for the addition of fluorescently conjugated annexin V into culture medium.

Since the fluorescently labeled annexin V is added to the medium and kept there during the monitoring period without any washing steps, it is possible that background fluorescence from the dye affects the detection sensitivity.[15] Recently, polarity-sensitive indicator of viability and apoptosis (pSIVA)-IANBD, an annexin-based, polarity-sensitive dye for PS, has become available.[22] This indicator has no fluorescence in solution; however, it fluoresces strongly upon binding to PS on the cell surface, because of the change of its microenvironment from aqueous solution to lipid cell membrane, and this binding is reversible. In the absence of PS on the cell surface, the dye is unbound (in solution); therefore, no background fluorescence is emitted, eliminating the need to wash out the unbound dye. This makes it ideal for live-cell imaging of PS externalization. In this paper, we report our results of PS externalization of mouse brain endothelial cells after radiosurgery using the live-cell imaging with the polarity-sensitive dye pSIVA-IANBD.

## Methods

### Materials

Black, 96-well cell-culture plates with a flat and clear bottom were obtained from Ibidi GmbH. The bEnd.3 cells were from the American Type Culture Collection, and pSIVA-IANBD apoptosis/viability microscopy kits were purchased from Imgenex. Attachment factor for cell culture was a product of Cell Systems. DMEM, fetal bovine serum (FBS), and 1% penicillin/streptomycin were from Invitrogen.

### Cell Culture

bEnd.3 cells, an immortalized cell line generated from mouse brain endothelium,[28] were grown according to the supplier's instructions in high-glucose DMEM containing 10% FBS, 4.5 g/L glucose, 3.7 g/L sodium bicarbonate, 4 mM glutamine, 100 U/ml penicillin, and 100 μg/ml streptomycin, at a pH of 7.4. Cells were maintained in a humid chamber at 37°C in an atmosphere of 95% air and 5% carbon dioxide in 75-$cm^2$ tissue-culture flasks. Confluent flasks were trypsinized and around 0.2% of the cells in

300 μl culture medium were seeded into individual wells (with a culture area of 0.55 $cm^2$) of a 96-well cell-culture plate precoated with attachment factor. The cells were allowed to grow for 1 day (about 20%–30% confluence) before undergoing irradiation.

### Cell Irradiation

A linear accelerator (LINAC; Elekta AB) at Macquarie University Hospital was used to irradiate the cells. The 96-well plate was CT scanned and a radiation-dose distribution was planned on the Elekta XiO planning system to deliver a differential dose (25 Gy, 15 Gy, 5 Gy, and < 0.5 Gy) to each of the 4 quadrants of the 96-well plate. Irradiation of the cells was carried out using 6-MV photons from anterior- and posterior-directed radiation fields. The cells in the area that received < 0.5 Gy were treated as a sham-radiation control. The culture medium was changed just before irradiation.

### Live-Cell Imaging

After irradiation, the dyes pSIVA-IANBD (1.5 μl) and propidium iodide (PI, 0.75 μl), in the apoptosis/viability microscopy kit, and the apoptosis-inducing agent camptothecin (final concentration 10 μM) were added to the corresponding wells. The 96-well plate containing the cells was then transferred to the automated stage of a Nikon Ti inverted epi-fluorescent microscope (Nikon Corp.) equipped with an environmental chamber set at 37°C. Humidified 5% carbon dioxide was supplied to the wells for the duration of the experiment. A ×40 phase objective (NA0.6) was used to collect transmission images, while pSIVA was detected in the FITC fluorescent channel (Ex 485 Em 521/13) and PI was detected in the Texas Red channel (Ex 607 Em 607/18). Two fields of view were selected in each well of triplicate wells, generating 6 fields of view for each radiation-dose group. Images were taken every 30 minutes at each field of view for 72 hours. The first image was taken 4 hours after irradiation. The experiment was repeated twice.

### Detection of PS Externalization and Cell Death

Manual counting by 2 of the authors independently (1 of whom was blinded to sample identity) of cell number and pSIVA- and PI-positive staining spots was performed in each of the 6 fields of view in each group to calculate the degrees of PS externalization and cell death for the cells exposed to different doses of radiation. Counting was performed on images taken at 4, 24, 49, and 74 hours after irradiation. The results shown are a representative analysis and are expressed as the ratios of positive counting/total cell number.

### Flow Cytometric Analysis of Cell Cycle

bEnd.3 cells were seeded into 75-$cm^2$ culture flasks, allowed to grow for 1 day (about 30% confluence), then irradiated using the linear accelerator, whereby cells received either 5-, 15-, or 25-Gy dose of radiation. Control cells were not exposed to radiation. Cells were harvested 3 days later, fixed in ice-cold 70% ethanol, and stained with PI (10 μl PI in 1 ml PBS containing 0.05% Triton X-100 and 100 μg ribonuclease A) for 30 minutes for detection of DNA. Flow cytometry analysis of cell cycle was performed on an LSR Fortessa X-20 cytometer (Becton, Dickinson and Co.). Data were acquired with DIVA software (version 8.1, Becton, Dickinson and Co.), collecting 10,000 events per sample with PI area fluorescence detected on a linear scale, and % forward (FWD)-area set to 0.40. Data were analyzed with CellQuest Pro (version 6.0; Becton, Dickinson and Co.), and with Modfit LT (version 3.2) for cell cycle analysis gating on single cells defined as those with proportional FWD-height versus FWD-area. The composite data figure was prepared using Adobe Illustrator CS6 (version 16.0.0; Adobe Systems Inc.).

### Statistical Analysis

Results are expressed as mean ± SD. Comparison of differences between test groups was made by unpaired two-tailed Student t-test. Differences were considered significant at $p < 0.05$.

## Results

### Effect of Radiation on Cell Proliferation

The cell confluence at the time of radiation treatment was 20%–30%, leaving enough room for the cells to proliferate during the 3-day incubation period under the microscope. The sham-radiated cells grew well, demonstrating the conditions in the chamber were appropriate for the cells. The cell number in each field of view was between 8 and 30.

The cell proliferation rates in the wells were radiation-dose dependent. The results were similar in the 2 separate experiments, and the rates from a representative run are shown in Fig. 1. In the sham-radiation wells, the number of cells in the fields of view increased by 140% by Day 3. Using this result as a control, radiation at a dose of 5 Gy significantly reduced the cell proliferation rate. The increase in cell number at Day 3 was less than 50% ($p < 0.01$). The higher radiation doses (15 Gy and 25 Gy) totally inhibited cell proliferation. The cell number was eventually reduced by around 20% at Day 3. The differences in percentage changes of cell numbers at Day 3 were not statistically significant between the groups receiving 15- or 25-Gy doses ($p = 0.72$), but both groups were significantly lower than the group treated with the 5-Gy dose and the sham-radiation controls ($p < 0.01$). The percentage change of cell number at Day 3 in the camptothecin-positive control group was similar between the groups treated with 15- or 25-Gy doses but significantly lower than the group treated with the 5-Gy dose and the sham-control groups ($p < 0.05$).

### Morphology Changes of the Cells After Irradiation

The low-density bEnd.3 cells at the time of irradiation exhibited a normal endothelial cell morphology with flattened and epithelial appearance, and some were elongated like fibroblasts (Fig. 2A and C). In comparison with sham radiation–treated cells, the irradiated cells showed distinct pseudopodial elongation with little or no spreading of the cell body and more cells with increased cytoplasmic volume. This was particularly apparent at late stages of the experiment and with higher radiation doses (Fig. 2C).

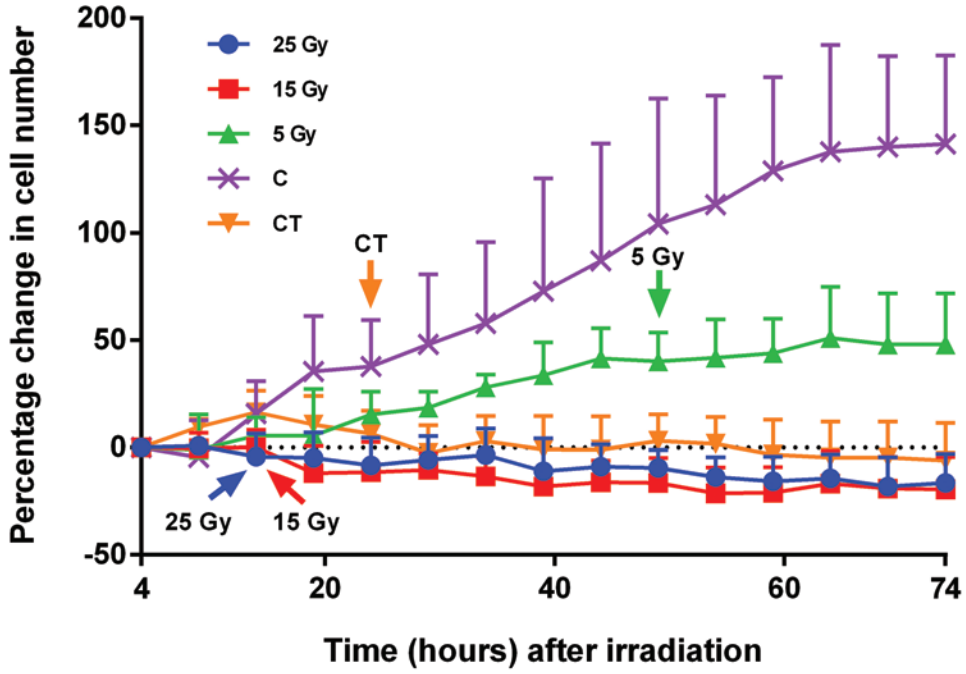


**FIG. 1.** Cell proliferation curves after exposure to radiation doses of 0, 5, 15, and 25 Gy. The results are expressed as the percentage changes of cell number relative to the initial cell number (4 hours), at different time points after irradiation in the relevant fields of view. The *arrows* indicate the time point where the differences in each group with sham-radiation control cells became statistically significant. C = sham-radiation control; CT = camptothecin.

### PS Externalization and Cell Death After Irradiation

In cells that underwent PS staining using pSIVA, only a few green spots could be seen per field of view at the beginning of imaging (4 hours after radiation exposure), and no significant differences in PS externalization could be detected in irradiated cells at any radiation-dose level in comparison with sham-radiation control cells (Fig. 2A and B). However, the percentages of pSIVA-positive cells, represented by the ratio of green spots to cell number in the corresponding fields, were significantly higher ($p = 0.04$) in the cells that received a 25- or 15-Gy dose of radiation 24 hours after treatment (Figs. 2A, 2B, and 3A). This effect was sustained until the end of the experiment (3 days), with the highest ratios at the last time point ($p < 0.01$). Radiation at 5 Gy did not induce significantly higher PS externalization compared with the sham-radiation control at any time points ($p > 0.15$). The effect of camptothecin on cell PS externalization was similar to that seen with the 25- and 15-Gy radiation doses. However, in comparison with radiation-treated cells, the increase in the pSIVA-positive cells in the second half of the incubation period was more notable in the camptothecin-treated cells. The results from a representative run are shown in Figs. 2 and 3.

The percentages of PI-positive cells, represented by the ratio of red spots to cell number in the corresponding fields, had a similar trend with the pSIVA-positive cells, although the values were much lower in all the radiation-dose groups at all time points (Figs. 2A and 3B). The percentages were significantly higher in 25- and 15-Gy treated cells at 24 hours after irradiation and later time points. In the cells treated with a 5-Gy dose of radiation and camptothecin, the percentage of PI-positive cells was significantly higher than sham-radiation control cells only at the end of the experiment (Figs. 2A and 3B).

Statistical analysis did not show any significant differences between 25- and 15-Gy radiation doses in cell pSIVA staining and PI staining at any time point. However, there were significant differences in pSIVA and PI staining between 15- and 5-Gy radiation doses at 49 and 74 hours postirradiation.

### Cell Cycle Analysis of the Irradiated Endothelial Cells

Irradiated bEnd.3 endothelial cells were also analyzed by flow cytometry. Here, the effect of irradiation was clearly evident, as even low-dose radiation (e.g., 5 Gy) resulted in a change in the cells FWD-area versus FWD-height dot-plot profile (Fig. 4A). Moreover, even in a simple ungated analysis, 15- and 25-Gy radiation doses appeared to alter the proportion of cells in G1 versus G2 of the cell cycle (Fig. 4A). These doses of radiation also more than doubled the number of polyploidy cells by 3 days (events right of the 2N peak in Fig. 4A). To confirm these results, a proper cell cycle analysis was performed by first gating on single cells, defined as cells that had a proportional FWD-height versus FWD-area ratio (region 1; R1, blue gate). The cell cycle analysis indicated that 48% of the cells had accumulated in the G2 phase of the cell cycle after a 25-Gy radiation dose, compared with just 19% in nonirradiated cells, with a similar effect after a 15-Gy radiation dose (23% G2) (Fig. 4B). Taken together, these data indicate that irradiation induces the growth arrest of bEnd.3 cells, with cells accumulating in the G2 phase of the cell cycle and with many cells becoming senescent as evident by their polyploidy state.

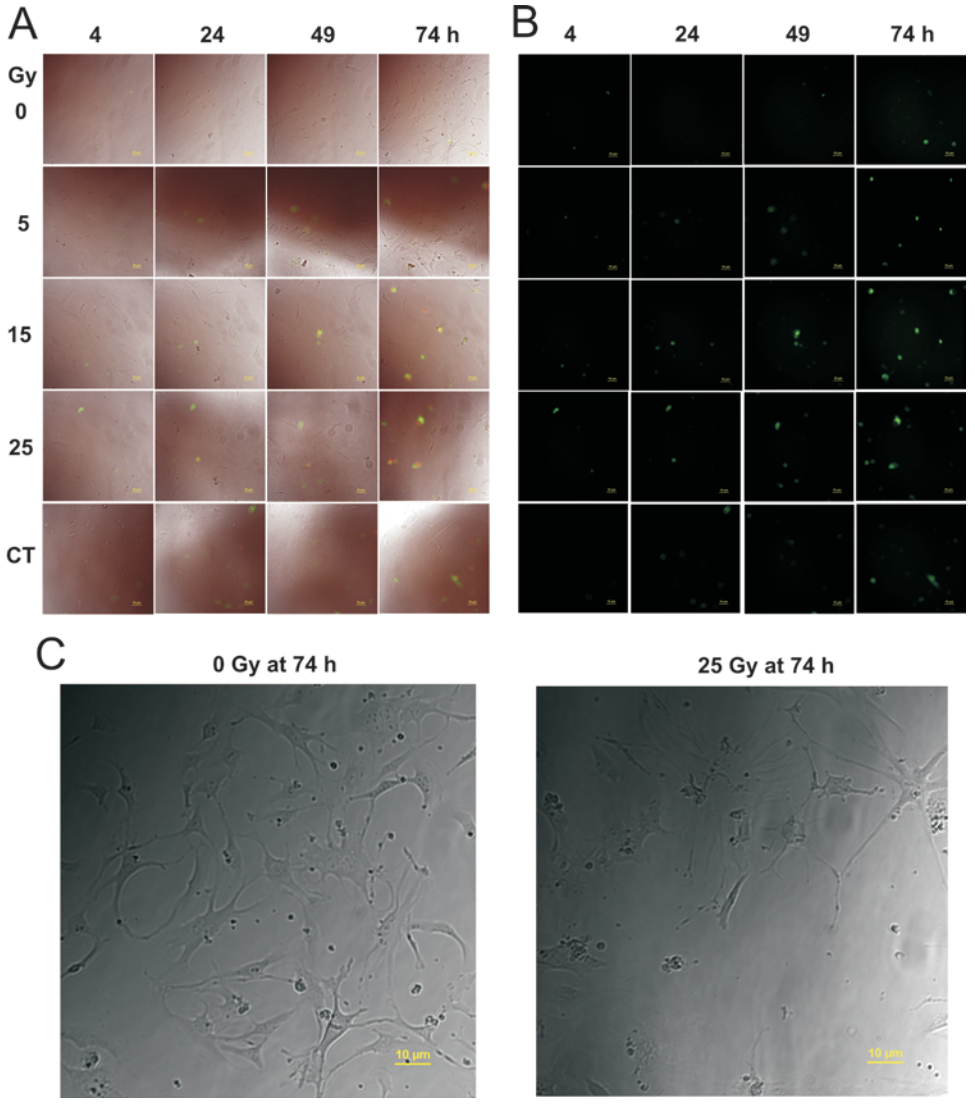


**FIG. 2.** Cell photomicrographs. **A and B:** Overlap images of pSIVA-positive and PI-positive cells under bright-field microscopy and pSIVA-positive spots only (green channel) (B) taken at 4, 24, 49, and 74 hours after exposure to 0-, 5-, 15-, and 25-Gy doses of radiation or treated by 10 μM camptothecin. **C:** Cell morphology at 74 hours after cells received sham radiation *(left)* or a 25-Gy radiation dose *(right)*. Scale bar = 10 μm.

## Discussion

The effect of ionizing radiation on cells is well documented.[24] It includes 2 main aspects: direct cellular damage through modification of macromolecules such as DNA and proteins, and indirect cellular damage through production of reactive oxidative species.[2] Depending on the level of damage, cell cycle arrest, DNA repair, senescence, or apoptosis will be initiated.[6] Endothelial cells are very sensitive to radiation.[8] Our previous studies revealed proinflammatory and thrombotic molecule changes on the surface of brain endothelial cells after ionizing radiation exposure.[25] The current study further confirmed that radiation at clinically relevant doses (15 and 25 Gy) has a clear effect on the bEnd.3 cells. Radiation at both doses totally inhibited the growth of the cultured cells, caused growth arrest and remarkable morphological changes, and induced significant PS externalization. Although the lower radiation dose (5 Gy) did not cause clear morphological changes or induce significant PS externalization, it clearly inhibited the growth of these cells.

Live-cell imaging takes advantage of the ability to sample data from essentially the same cells (identical fields of view) at different points in time postradiation exposure. This allowed for easy tracking of proliferation of individual cells but only for a limited number of cells (i.e., those within the imaged fields). However, flow cytometry analysis permits analysis of significantly more cells (10,000 cells or more) and additionally defined that irradiation caused the accumulation of cells in the G2 phase of the cell cycle. The results are consistent with previous reports on ionizing radiation effect on cells.[19,23,41] Thus, the radiation induced a growth inhibition that was largely due to cell cycle inhibition, senescence, and/or cell death.

Since the distribution of PS on the cell surface is uneven and apoptotic cells may break into several pieces,[46]

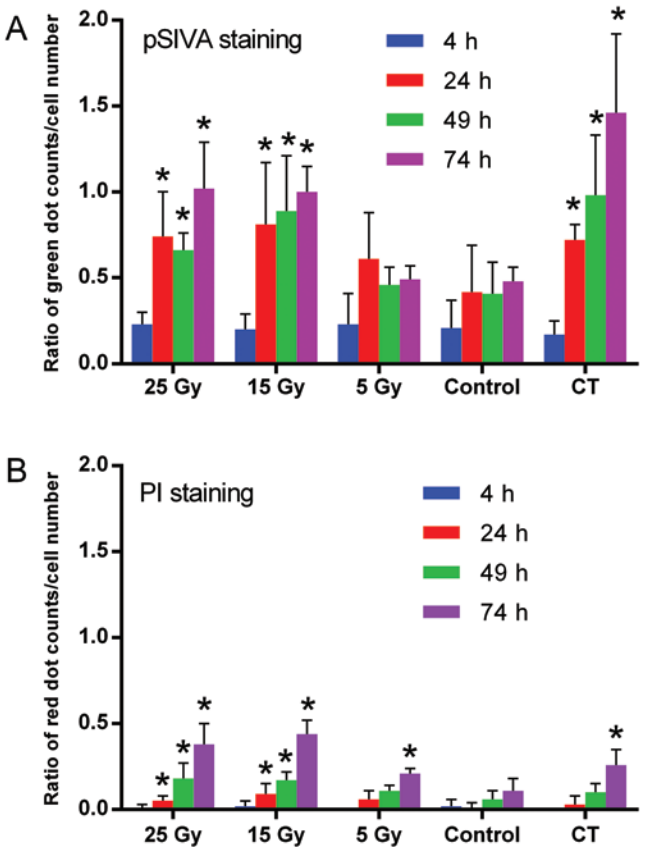


**FIG. 3.** Bar graphs of colored dot counts to cell number in cell cultures stained with pSIVA and PI. **A and B:** The ratio of pSIVA-positive spots (A) and the ratio of PI-positive spots (B) to cell number in the cells exposed to 25-, 15-, 5-, and 0-Gy radiation doses, and the cells treated with camptothecin at different time points. *Asterisk* indicates statistically significant differences in comparison with 0-Gy controls. h = hour.

1 cell may have several PS- or PI-positive staining spots. The ratio in Fig. 3 might not exactly represent the percentage of positive cells but should be an indicator of the degree of PS externalization or cell death.

These results may have physiological relevance in understanding the effect of radiosurgery on AVMs. The cellular changes of the endothelium in AVMs may be involved in the obliteration process after radiosurgery. The PS expressed on the endothelial cell surface has the potential to induce thrombus formation.[5] Of more immediate clinical relevance, the molecule may also represent a valid radiation-induced marker for vascular targeting, although more work is required to understand its detailed expression profile after irradiation. Detection of PS expression on AVM endothelium after radiosurgery in a rat AVM model, using an in vivo imaging technique, is underway in our laboratory. Preliminary data suggest that selective induction of PS externalization by ionizing radiation on endothelium of AVM tissues can be achieved in vivo (data not shown).

This study did not find obvious differences in biological effects of 15- and 25-Gy radiation doses on the bEnd.3 cells in cell proliferation, morphological changes, and PS externalization. The results suggest that the dose of 15 Gy may be adequate to induce the necessary changes in endothelial cells for vascular targeting. However, this does not mean a 15-Gy dose of radiation is enough for vascular obliteration in AVMs. Clinical work has demonstrated that a margin dose of 16–25 Gy is necessary to achieve a satisfactory occlusion rate.[10,44] More work with smaller titrations of radiation doses and larger animal numbers per group is required to find the optimal radiation dose for vascular targeting. Given that high doses of radiation, including current clinical doses, can lead to off-target effects and late radiation necrosis,[27] it would be clinically very significant if lower radiation doses could induce sufficient molecular changes on the endothelial surface for vascular targeting.

Live-cell imaging can monitor molecular changes on the cell surface in real time without the need to process the cells except for the addition of the dyes into the culture medium. It is designed to observe the same sets of cells in each field of view at different time points, eliminating the experimental errors caused by the variation among the cells. It also has the capacity to monitor the changes of a single cell. Up to a few hundred fields of view across the cell culture plate can be monitored in just 1 experiment. With the radiation dose designed to deliver the desired doses to different parts or wells of the plate, this technique can detect the effects of different radiation doses on the cells in real time with just 1 run. However, there were some drawbacks with the system that we used. The bright-field image quality was affected near the edges of the narrow wells, and condensation on the lid altered the brightness of the images over time. In this system, the environmental chamber lid could not be removed once mounted onto the microscope; therefore the culture medium could not be changed during the imaging process, limiting the monitoring period to a maximum of 3 days in this study. The results cannot reveal whether all the PS-positive cells will eventually die or can recover or be rescued to normal cells. The expression of PS on the cell surface increased with time during the monitoring period. No peak expression time was identified. Nevertheless, large amounts of information regarding the changes of the cells during the monitoring period can be obtained if the conditions are carefully controlled and appropriate control cells are included in the experiments.

Naturally, it is a limitation of all in vitro investigations that the microenvironment for the cultured cells is different from the in vivo conditions. There are no other cells to interact with these cells, such as macrophages to get rid of abnormal cells.[21] The cells in vivo do not have the space to proliferate. Nevertheless, this in vitro study provides valuable insight into what might happen in vivo and, thus, forms a strong foundation for designing in vivo work in the future.

## Conclusions

Ionizing radiation causes remarkable cellular changes in endothelial cells. Significant PS externalization is induced by radiation at doses of 15 Gy or higher, concomitant with a block in the cell cycle. Radiation-induced markers/targets may have high discriminating power to be harnessed in vascular targeting for AVM treatment.

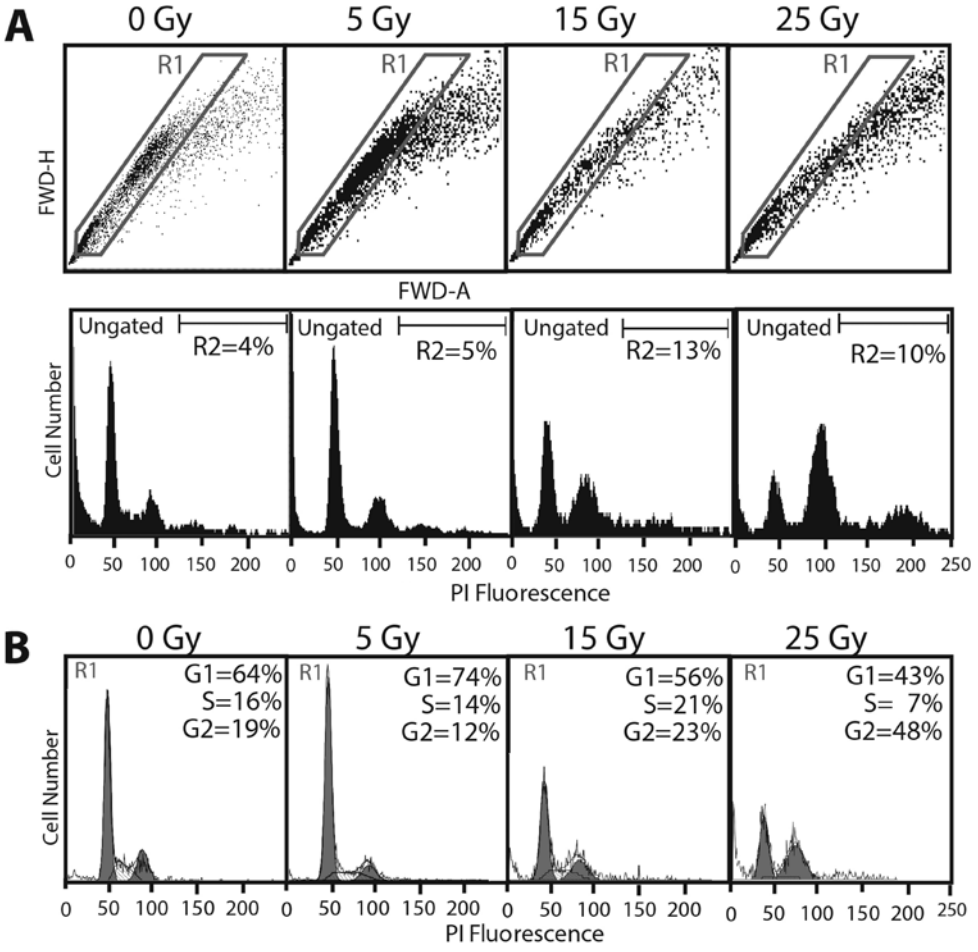


**FIG. 4.** Flow cytometry analysis of irradiated bEnd.3 cells. **A:** The proportional size (FWD-H [forward height] and FWD-A [forward area]) and nuclear content represented by intracellular PI fluorescence of permeabilized bEnd.3 cells 3 days after irradiation. **B:** Cell cycle analysis of single cells (R1 gate, as defined in A) after irradiation, indicating the percentage of cells in the G1, S, or G2 phase of the cell cycle. Data shown are representative of independently repeated experiments.

## Acknowledgments

This study received financial support from the National Health and Medical Research Council of Australia (APP1047302). Dr. Zhenjun Zhao is a recipient of the Macquarie University Vice-Chancellor's Innovation Fellowship.

## References

1. Barr JC, Ogilvy CS: Selection of treatment modalities or observation of arteriovenous malformations. **Neurosurg Clin N Am 23:**63–75, 2012
2. Brown KR, Rzucidlo E: Acute and chronic radiation injury. **J Vasc Surg 53 (1 Suppl):**15S–21S, 2011
3. Chang SD, Shuster DL, Steinberg GK, Levy RP, Frankel K: Stereotactic radiosurgery of arteriovenous malformations: pathologic changes in resected tissue. **Clin Neuropathol 16:**111–116, 1997
4. Corso CD, Ali AN, Diaz R: Radiation-induced tumor neoantigens: imaging and therapeutic implications. **Am J Cancer Res 1:**390–412, 2011
5. Dombroski D, Balasubramanian K, Schroit AJ: Phosphatidylserine expression on cell surfaces promotes antibody-dependent aggregation and thrombosis in beta2-glycoprotein I-immune mice. **J Autoimmun 14:**221–229, 2000
6. Eriksson D, Stigbrand T: Radiation-induced cell death mechanisms. **Tumour Biol 31:**363–372, 2010
7. Fabisiak JP, Borisenko GG, Kagan VE: Quantitative method of measuring phosphatidylserine externalization during apoptosis using electron paramagnetic resonance (EPR) spectroscopy and annexin-conjugated iron. **Methods Mol Biol 1105:**613–621, 2014
8. Fajardo LFLG: Ionizing radiation and the endothelium, in Rubin P, Constine LS, Marks LB, et al (eds): **Late Effects of Cancer Treatment on Normal Tissues.** Berlin: Springer, 2008
9. Flickinger JC, Kano H, Niranjan A, Kondziolka D, Lunsford LD: Dose selection in stereotactic radiosurgery. **Prog Neurol Surg 27:**49–57, 2013
10. Flickinger JC, Pollock BE, Kondziolka D, Lunsford LD: A dose-response analysis of arteriovenous malformation obliteration after radiosurgery. **Int J Radiat Oncol Biol Phys 36:**873–879, 1996
11. Fokas E, Henzel M, Wittig A, Grund S, Engenhart-Cabillic R: Stereotactic radiosurgery of cerebral arteriovenous malformations: long-term follow-up in 164 patients of a single institution. **J Neurol 260:**2156–2162, 2013
12. Friedman WA, Blatt DL, Bova FJ, Buatti JM, Mendenhall WM, Kubilis PS: The risk of hemorrhage after radiosurgery for arteriovenous malformations. **J Neurosurg 84:**912–919, 1996
13. Friedman WA, Bova FJ, Bollampally S, Bradshaw P: Analysis of factors predictive of success or complications

in arteriovenous malformation radiosurgery. **Neurosurgery 52:**296–308, 2003
14. Han PP, Ponce FA, Spetzler RF: Intention-to-treat analysis of Spetzler-Martin grades IV and V arteriovenous malformations: natural history and treatment paradigm. **J Neurosurg 98:**3–7, 2003
15. Hori Y, Norinobu T, Sato M, Arita K, Shirakawa M, Kikuchi K: Development of fluorogenic probes for quick no-wash live-cell imaging of intracellular proteins. **J Am Chem Soc 135:**12360–12365, 2013
16. Jeffree RL, Stoodley MA: Postnatal development of arteriovenous malformations. **Pediatr Neurosurg 45:**296–304, 2009
17. Jeggo P, Lavin MF: Cellular radiosensitivity: how much better do we understand it? **Int J Radiat Biol 85:**1061–1081, 2009
18. Jöst E, Roos WP, Kaina B, Schmidberger H: Response of pancreatic cancer cells treated with interferon-alpha or beta and co-exposed to ionising radiation. **Int J Radiat Biol 86:**732–741, 2010
19. Jun HJ, Kim YM, Park SY, Park JS, Lee EJ, Choi SA, et al: Modulation of ionizing radiation-induced G2 arrest by cyclooxygenase-2 and its inhibitor celecoxib. **Int J Radiat Oncol Biol Phys 75:**225–234, 2009
20. Karunanyaka A, Tu J, Watling A, Storer KP, Windsor A, Stoodley MA: Endothelial molecular changes in a rodent model of arteriovenous malformation. **J Neurosurg 109:**1165–1172, 2008
21. Kearns MT, Dalal S, Horstmann SA, Richens TR, Tanaka T, Doe JM, et al: Vascular endothelial growth factor enhances macrophage clearance of apoptotic cells. **Am J Physiol Lung Cell Mol Physiol 302:**L711–L718, 2012
22. Kim YE, Chen J, Chan JR, Langen R: Engineering a polarity-sensitive biosensor for time-lapse imaging of apoptotic processes and degeneration. **Nat Methods 7:**67–73, 2010
23. Landsverk KS, Patzke S, Rein ID, Stokke C, Lyng H, De Angelis PM, et al: Three independent mechanisms for arrest in G2 after ionizing radiation. **Cell Cycle 10:**819–829, 2011
24. Li L, Story M, Legerski RJ: Cellular responses to ionizing radiation damage. **Int J Radiat Oncol Biol Phys 49:**1157–1162, 2001
25. Liu S, Sammons V, Fairhall J, Reddy R, Tu J, Duong TT, et al: Molecular responses of brain endothelial cells to radiation in a mouse model. **J Clin Neurosci 19:**1154–1158, 2012
26. Liu T, Zhu W, Yang X, Chen L, Yang R, Hua Z, et al: Detection of apoptosis based on the interaction between annexin V and phosphatidylserine. **Anal Chem 81:**2410–2413, 2009
27. Monaco EA III, Niranjan A, Kano H, Flickinger JC, Kondziolka D, Lunsford LD: Management of adverse radiation effects after radiosurgery for arteriovenous malformations. **Prog Neurol Surg 27:**107–118, 2013
28. Montesano R, Pepper MS, Möhle-Steinlein U, Risau W, Wagner EF, Orci L: Increased proteolytic activity is responsible for the aberrant morphogenetic behavior of endothelial cells expressing the middle T oncogene. **Cell 62:**435–445, 1990
29. Nataraj A, Mohamed MB, Gholkar A, Vivar R, Watkins L, Aspoas R, et al: Multimodality treatment of cerebral arteriovenous malformations. **World Neurosurg 82:**149–159, 2014
30. Nguyen T, Hsu W, Lim M, Naff N: Delivery of stereotactic radiosurgery: a cross-platform comparison. **Neurol Res 33:**787–791, 2011
31. Pollock BE, Flickinger JC: Modification of the radiosurgery-based arteriovenous malformation grading system. **Neurosurgery 63:**239–243, 2008
32. Puigvert JC, de Bont H, van de Water B, Danen EH: High-throughput live cell imaging of apoptosis. **Curr Protoc Cell Biol 47:**18.10.1–18.10.13, 2010
33. Reddy R, Hong Duong TT, Fairhall JM, Smee RI, Stoodley MA: Durable thrombosis in a rat model of arteriovenous malformation treated with radiosurgery and vascular targeting. **J Neurosurg 120:**113–119, 2014
34. Riquier H, Wera AC, Heuskin AC, Feron O, Lucas S, Michiels C: Comparison of X-ray and alpha particle effects on a human cancer and endothelial cells: survival curves and gene expression profiles. **Radiother Oncol 106:**397–403, 2013
35. Roy L, Gruel G, Vaurijoux A: Cell response to ionising radiation analysed by gene expression patterns. **Ann Ist Super Sanita 45:**272–277, 2009
36. Schneider BF, Eberhard DA, Steiner LE: Histopathology of arteriovenous malformations after gamma knife radiosurgery. **J Neurosurg 87:**352–357, 1997
37. Stoodley MA, Weir BKA: Aneurysms and arteriovenous malformations, in Asbury A, McKhann G, McDonald W, et al (eds): **Diseases of the Nervous System: Clinical Neuroscience and Therapeutic Principles, ed 3.** Cambridge: Cambridge University Press, 2002, pp 1392–1404
38. Storer K, Tu J, Karunanayaka A, Smee R, Short R, Thorpe P, et al: Coadministration of low-dose lipopolysaccharide and soluble tissue factor induces thrombosis after radiosurgery in an animal arteriovenous malformation model. **Neurosurgery 61:**604–611, 2007
39. Storer KP, Tu J, Karunanayaka A, Morgan MK, Stoodley MA: Inflammatory molecule expression in cerebral arteriovenous malformations. **J Clin Neurosci 15:**179–184, 2008
40. Storer KP, Tu J, Karunanayaka A, Morgan MK, Stoodley MA: Thrombotic molecule expression in cerebral vascular malformations. **J Clin Neurosci 14:**975–980, 2007
41. Szymczyk KH, Shapiro IM, Adams CS: Ionizing radiation sensitizes bone cells to apoptosis. **Bone 34:**148–156, 2004
42. van Beijnum J, van der Worp HB, Buis DR, Al-Shahi Salman R, Kappelle LJ, Rinkel GJ, et al: Treatment of brain arteriovenous malformations: a systematic review and meta-analysis. **JAMA 306:**2011–2019, 2011
43. Vincent AM, Maiese K: Direct temporal analysis of apoptosis induction in living adherent neurons. **J Histochem Cytochem 47:**661–672, 1999
44. Wegner RE, Oysul K, Pollock BE, Sirin S, Kondziolka D, Niranjan A, et al: A modified radiosurgery-based arteriovenous malformation grading scale and its correlation with outcomes. **Int J Radiat Oncol Biol Phys 79:**1147–1150, 2011
45. Wong K, Li X, Ma Y: Paraformaldehyde induces elevation of intracellular calcium and phosphatidylserine externalization in platelets. **Thromb Res 117:**537–542, 2006
46. Xiong C, Brewer K, Song S, Zhang R, Lu W, Wen X, et al: Peptide-based imaging agents targeting phosphatidylserine for the detection of apoptosis. **J Med Chem 54:**1825–1835, 2011

## Disclosure

The authors report no conflict of interest concerning the materials or methods used in this study or the findings specified in this paper.

## Author Contributions

Conception and design: Zhao, Johnson, Grace, Ukath, Stoodley. Acquisition of data: Zhao, Johnson, Chen, Grace, Ukath, Lee, McRobb, Sedger. Analysis and interpretation of data: Zhao, Johnson, McRobb, Sedger, Stoodley. Drafting the article: Zhao, Sedger. Critically revising the article: Johnson, Lee, McRobb, Sedger, Stoodley. Reviewed submitted version of manuscript: all authors. Approved the final version of the manuscript on behalf of all authors: Zhao. Statistical analysis: Zhao. Study supervision: Zhao, Stoodley.

## Correspondence

Zhenjun Zhao, Faculty of Medicine and Health Sciences, F10A, 2 Technology Place, Macquarie University, Sydney, NSW 2109 Australia. email: zhenjun.zhao@mq.edu.au.